Versatile Compact Verilog-A Model of a STT-MTJ

1st L. Durieux
ICube Laboratory,
University of Strasbourg
Strasbourg, France
laura.durieux@unistra.fr

2nd H. Nicolas
Swiss Nanoscience Institute, School of Life Sciences and ICube Laboratory
University of Basel, University of Applied Sciences and University of Strasbourg
Basel, Muttenz and Strasbourg, Switzerland and France
hugo.nicolas@fhnw.ch

3rd R.C. Sousa
Spintec, CEA
CNRS, University of Grenoble Alpes
Grenoble, France
ricardo.sousa@cea.fr

4th J. Pascal
Swiss Nanoscience Institute and School of Life Sciences
University of Basel, University of Applied Sciences
Basel, Muttenz, Switzerland
joris.pascal@fhnw.ch

5th J.-B. Kammerer
ICube Laboratory
University of Strasbourg
Strasbourg, France
jb.kammerer@unistra.fr

***Abstract*—The development of MTJ-based systems necessitates the development of efficient compact models. Despite the existence of numerous compact models, no model has been developed that is both versatile and extendable to other spintronic devices while maintaining a reasonable level of complexity to minimize the simulation time. In this paper, we propose a tunable MTJ model comprising ferromagnetic layers and electrical compact models interconnected to facilitate reuse in the modeling of numerous other spintronic devices. The model incorporates phenomena such as the spin transfer torque, the spin orbit torque, as well as magnetic and electrical noise. The model's behavior reflects that of actual MTJs, thereby enabling accurate and efficient simulations of MTJ-based circuits.**

***Index Terms*—Compact Model, Magnetometer, MRAM, MTJ, SOT, spintronic, STT, Verilog-A**

I. Introduction

Spintronic devices have a wide range of applications and are increasingly used. Among the most extensively studied spintronic devices are the Magnetic Tunnel Junctions (MTJs), which are frequently utilized as magnetic sensors or as memory cells for non-volatile Magnetic Random-Access Memories (MRAM) [1], [2]. MTJs have also been utilized in configurable or low-power circuits [3], [4] and neuromorphic computing systems [5]. To study the behavior of such circuits, micromagnetic simulators are often employed, though these simulations can be time- and resource-consuming. In recent years, there has been a focus on developing compact models for MTJs to streamline and simplify the simulation of MTJ-based circuits. One of the earliest compact models, which took into account the dynamic behavior of the magnetizations of the ferromagnetic (FM) layers as well as the electrical behavior of the MTJ, was developed in VHDL-AMS several years ago [6]–[8]. This model incorporates numerous MTJ phenomena, including layer magnetization, spin-dependent tunneling, magnetic coupling, and demagnetizing fields. Subsequent studies have proposed a multitude of models, incorporating either the spin transfer torque (STT) [1] or the spin orbit torque (SOT) effects [9]. The majority of the proposed simulation models have focused on magnetic RAMs. To the best of our knowledge, no model implementing both STT and SOT effects has been developed thus far. To address the aforementioned limitations, we have developed a compact MTJ model that incorporates both STT and SOT effects, and noise. Notably, the model incorporates magnetic noise, which is known to induce stochastic behavior in the magnetization reversal of the FM layers. The model has been fully written in Verilog-A, a language that is compatible with most SPICE-like simulators. The first section is dedicated to the presentation of the fundamentals of MTJs. The subsequent section provides a comprehensive overview of the equations employed in our compact model. The design of the full Verilog-A model is then presented in section III. In the last section, simulation results of the behavior of the MTJ as well as simulations of a MTJ-based magnetometer are presented before the conclusion.

II. STT-MTJ model

A. Basics on MTJs

Magnetic tunnel junctions (MTJs) consist of two ferromagnetic (FM) layers separated by a thin layer of insulating and non-magnetic material. The insulating layer allows the transfer of electrons between the two FM layers through the tunnel effect. The transmission rate is influenced by the relative orientation of the magnetizations of both layers. Consequently, a high MTJ resistance is observed when the magnetizations of both layers are in opposite directions, and a low resistance is measured when they are parallel. The magnetic reversal can be induced by several mechanisms, including the application of a magnetic field, STT, or SOT.

B. Global model architecture

Our MTJ model consists of two compact magnetization models to describe the behaviors of the two FM layers and an electrical model to evaluate the conductance of the junction. Our magnetization model is based on a slightly modified Landau-Lifshitz-Gilbert (LLG) equation with a continuous control of the norm of the magnetization vector as explained

in [6], [7]. The electrical part of our MTJ model is inspired by this work [8].

In the following subsections, we highlight the additional parts of the equation that model the STT and SOT effects. The magnetic and electrical noises have also been added to model the stochastic behavior of actual MTJs and to accurately describe the effect of noise on the behavior of the MTJ.

C. Electrical model

The electrical model of the MTJ used in this work is based on a simplified version of the free electron model [7], [8]. The conductance G of the MTJ changes according to the conductances of the antiparallel and parallel states, G_{AP} and G_P respectively. Since the actual conductance of the MTJ depends on the relative orientation of both magnetization vectors, it is evaluated thanks to the scalar product of the normalized magnetizations of both FM layers [8]:

$$G = \frac{(G_P + G_{AP}) + (G_P - G_{AP})(\vec{m} \cdot \vec{m}')}{2} \tag{1}$$

where $\vec{m}$ and $\vec{m}'$ are the normalized magnetization vectors of both FM layers. Based on the conductance, the total current flowing through the MTJ can be calculated. More details are given in [8].

D. Magnetization model

We started with a modified LLG equation. In addition to the Zeeman and damping terms, this modified LLG equation includes a term responsible for the gyroscopic motion of the magnetization around the easy axis of the modeled FM layer and a correction term compensating for the accumulation of numerical errors induced by the integration algorithm used in circuit simulators [6]:

$$\begin{aligned} \frac{d\vec{M}}{dt} =& -\gamma \cdot \mu_0 \cdot \vec{M} \times \vec{H}_{eff} \\ &+ \frac{\alpha}{M_s} \cdot \vec{M} \times \frac{d\vec{M}}{dt} \\ &- \gamma \cdot \frac{2 \cdot K}{M_s^2} \cdot (\vec{M} \cdot \vec{u}_{ea}) \cdot (\vec{M} \times \vec{u}_{ea}) \\ &+ \frac{1}{\tau} \cdot (1 - \|\vec{m}\|) \cdot \vec{M} \end{aligned} \tag{2}$$

where $\gamma = g \cdot (q/2 \cdot m_e)$ with g the Landé factor depending on the material, m_e the mass of the electron, q the elementary charge, μ_0 the vacuum permeability, K the anisotropic constant which depends on the material, M_s the saturation magnetization of the material, α the damping factor, τ the time constant of the norm control term and $\vec{u}_{ua}$ a unity vector defining the direction of the easy axis. $\vec{H}_{eff}$ is the effective field seen by the considered FM layer:

$$\vec{H}_{eff} = \vec{H} + \vec{H}_D + C_p \cdot \vec{M}' \tag{3}$$

where $\vec{H}$ is the external magnetic field, $\vec{H}_D$ is the demagnetizing field equals to $-G_D \cdot \vec{M}$ with G_D the demagnetizing tensor depending on the geometry of the considered layer [6]. C_p is the magnetic coupling coefficient, and $\vec{M}'$ represents the magnetization vector of the other layer.

E. STT and SOT effects

STT effect allows the switching of the magnetization vector by the injection of a strong enough spin polarized current. To model this phenomenon, we added a term to the $\frac{d\vec{M}}{dt}$ dynamic magnetization model described earlier in the paper:

$$\frac{d\vec{M_{STT}}}{dt} = a_j \cdot J \cdot \vec{M} \times (\vec{M} \times \vec{M}') \tag{4}$$

where a_j is the STT coefficient, J the current density flowing through the junction, and $\vec{M}$ and $\vec{M}'$ are the magnetization vectors of the modeled layer and the other layer respectively.

The SOT phenomenon does not manifest in STT-MTJs. However, the objective was to ensure the FM layer model's generalizability to facilitate its use in other spintronic device models. To this end, we incorporated a second term into our dynamic magnetization model to account for the SOT:

$$\frac{d\vec{M}_{SOT}}{dt} = b_j \cdot J \cdot (\vec{M} \times \vec{M}') \tag{5}$$

where b_j is the SOT coefficient. Finally, these two last terms are added to equation (2) to determine the derivative over time of the magnetization vector which is numerically integrated by the simulator.

F. Noise

1) Magnetic noise: In order to obtain a more realistic model, we incorporated magnetic noise, which is responsible for the stochastic behavior of the magnetization reversal. This stochasticity is of major importance since it directly determines the switching probability of a FM layer versus the voltage applied across the MTJ. This probability is critical in determining the minimum voltage required to ensure correct bit writing in a STT-MTJ MRAM cell, as well as the resolution of a MTJ-based magnetometer.

First, we took into consideration the thermal and $\frac{1}{f}$ magnetic noises defined by their noise spectral power densities [10]:

$$S_M = \frac{4 \cdot k_B \cdot T \cdot \mu_0 \cdot \alpha}{\Omega \cdot \gamma \cdot M_S} + \frac{2 \cdot B_{sat} \cdot \beta_f}{\Omega \cdot f} \tag{6}$$

where Ω is the volume of the considered ferromagnetic layer of the MTJ, T is the temperature, k_B is the Boltzmann constant, B_{sat} is the saturation field of the free layer and β_f an empirical parameter which can be extracted from the measured noise spectrum of the MTJ. The random signal induced by that noise spectral density is added to the effective field H_{eff} of equation (2).

2) Electrical noise: The electrical noise, composed of thermal noise, shot noise, and flicker noise [10], is also included in this model. Thermal and shot noises S_{V_t} were represented by the following equation:

$$\begin{aligned} S_{V_t} =& F \cdot 2 \cdot e \cdot I \cdot R^2 \cdot coth\left(\frac{e \cdot V}{2 \cdot k_B \cdot T}\right) \\ &+ (1 - F) \cdot 4 \cdot k_B \cdot T \cdot R \end{aligned} \tag{7}$$

where V is the voltage across the MTJ junction, F is the Fano factor described in [11]. If the MTJ experience a full shot noise

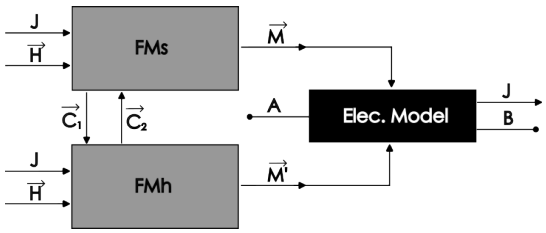

Fig. 1. Ferromagnetic and electrical models connected together to form the full STT-MTJ model. $\vec{H}$ is the external magnetic field represented as a 3D vector. J is the current density flowing through the MTJ. $\vec{M}$ and $\vec{M}'$ are the magnetization layer of the soft and hard ferromagnetic layers respectively. A and B are the terminals of the MTJ. Only A, B and $\vec{H}$ represent the external terminals of the model.

then $F = 1$. $R = \frac{1}{G}$ is the resistance, I is the current flowing through the junction, and e is the electronic charge.

Finally, the $\frac{1}{f}$ electronic noise S_{V_f} was implemented using the following equation:

$$S_{V_f} = \frac{\alpha_H \cdot V^2}{S \cdot f^\beta} \tag{8}$$

where S is the area of the MTJ, α_H is the Hooge parameter that depends on several parameters such as the material type, its quality, or the temperature. It is an empirical parameter that can be measured as described in the following papers [12]. β is a fitting parameter that can fluctuates between 0.6 and 2.0.

3) Full STT-MTJ model: The complete STT-MTJ model is obtained by coupling two FM layer models and one electrical model, as illustrated in Fig.1. It has three terminals, of which two represent the electrical terminals, which in turn represent the electrodes of the MTJ. The third terminal is used to set the external magnetic field.

The STT-MTJ model has 32 parameters, i.e. 10 parameters for each FM layer model and 12 for the electrical model. The parameters of a FM layer model are the anisotropy constant K, the saturation magnetization M_s, the damping factor α, the demagnetizing tensor, the easy axis orientation, the STT and SOT coefficients a_j and b_j, the magnetic coupling factor, and the magnetic noise parameters. The parameters of the electrical part are the area of the junction, the surfacic capacitance, two times three polynomial coefficients to describe the non-linear current versus voltage of the junction in both parallel and antiparallel configurations [8], and the electrical noise parameters.

III. Simulation Results

All simulations were conducted within the Cadence® environment using the Spectre® simulator. To validate the model, the simulations were divided into three sections, each with a specific objective. 1) validate the STT-MTJ model and demonstrate that the simulated behavior is correct and conforms to the results given in the papers we most inspired from [6]–[8]; 2) validate the implementations of the noises; 3) demonstrate the versatility of the that model by simulating the behavior of an actual MTJ-based magnetometer [13]. In the absence of the SOT effect in the STT-MTJ, this effect has been removed by setting the parameter b_j to zero.

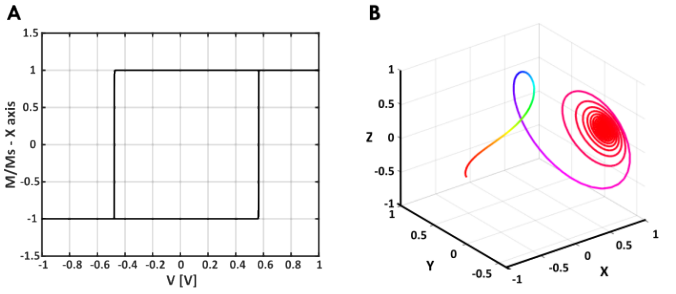

Fig. 2. A: Normalized easy-axis component of the magnetization versus applied potential. B: Trajectory of the normalized magnetization of the soft FM layer during a reversal.

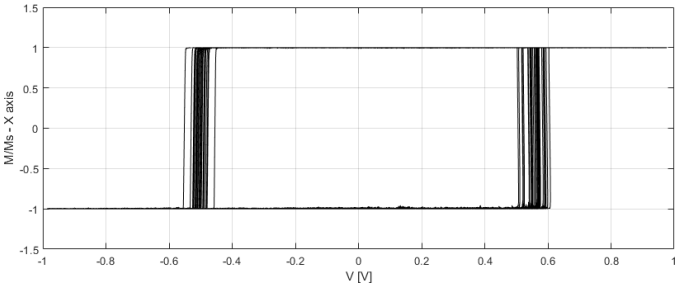

Fig. 3. Stochasticity induced by the magnetic noise. The magnetization vector is normalized.

A. STT-MTJ behavior

The simulations made to evaluate and validate our model were conducted with a ± 1 V sinusoidal voltage at 100 kHz applied across a STT-MTJ with a diameter of 64 nm. Given the predominantly linear nature of the current versus voltage characteristic at low bias voltage, the tunnel magnetoresistance bias voltage dependence was not considered. The parallel and antiparallel resistances were set to 5 kΩ and 10 kΩ respectively. The coupling coefficient was set to 0.1.

As illustrated in Fig.2-A, the hysteretic behavior of the magnetization in the soft layer is evident. Furthermore, Fig.2-B illustrates the trajectory of the normalized magnetization vector during a magnetization reversal, thereby demonstrating its conformity with the LLG model.

B. Magnetic noise induces stochasticity

In a subsequent series of simulations, it was demonstrated that magnetic noise models introduce stochasticity into the switching of the magnetization vector, as illustrated in Fig.3. Consequently, the switching voltages of the modeled STT-MTJ can fluctuate by up to ±50 mV around their nominal values.

C. STT-MTJ integrated into a circuit

In addition, an evaluation of the model was conducted by utilizing it for the simulation of the behavior of a STT-MTJ-based magnetometer. The circuit depicted in Fig.4 enables the detection of resistance fluctuations in a MTJ driven by

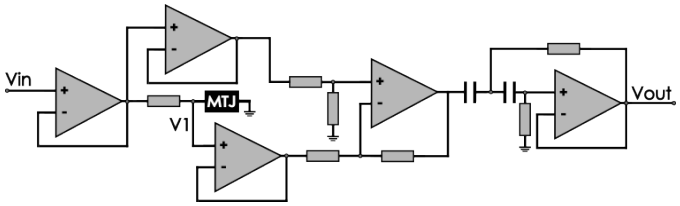

Fig. 4. Circuit allowing the detection of switching events used in [13].

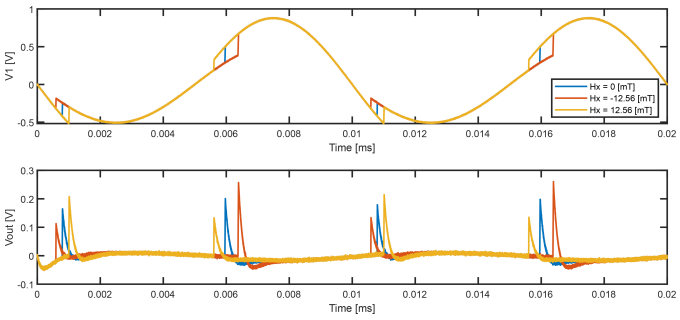

Fig. 5. Simulation results of the circuit used to detect the reversals of the magnetization vector depending on the intensity of the magnetic field on the out-of-plane axis (Hx). On top the voltage accross the MTJ (V1) is shown. The output voltage is shown on the bottom part.

a sine wave, utilizing the four left operational amplifiers. The signal subsequently passes through a Sallen-Key high-pass filter, which generates a pulse at each magnetic reversal [13]. We performed simulations for different magnetic fields (-12.56 mT, 0 mT, 12.56 mT) to evaluate the sensitivity of this magnetometer. As illustrated in Fig.5, the magnetic field exerts an influence on the timing of the switching events, thereby affecting the instants at which the pulses appear in the output signal. Consistent with the actual prototype, the time shift of the pulses is measured to be near 90 ns/mT. Additionally, it was observed that the standard deviation of the distribution of the switching events contributes to a noise level of 2.89 µT/$\sqrt{Hz}$. These results align closely with experimental data obtained on an actual STT-MTJ utilized as a sensing element in a fluxgate-like magnetometer [13].

IV. Conclusion

A versatile and tunable Verilog-A MTJ model has been presented in this paper. The magnetization model used to model the FM layers is inspired from previous works [6]–[8] using a modified LLG equation, augmented to encompass additional phenomena such as STT, SOT, and noise. The new obtained model allows to accurately simulate the precession of the magnetization vector, the impact of the magnetic noise on the switching behavior, and the STT phenomenon. In particular, the stochasticity in the magnetization reversal, which is a key aspect in MTJ-based system simulations, is well described. It overall shows consistent results when linked to a circuit compared to results obtained from an actual MTJ-based magnetometer [13]. Specifically, the simulated signal-to-noise ratio is in perfect agreement with the one measured on the actual prototype. This model has the potential to simulate the behavior of a MRAM cell or any other MTJ-based system. Even if in the STT-MTJ model presented in this paper the parameter b_j which defines the strength of the SOT effect has been set to zero, this effect has been included in the FM layer model. Consequently, this FM layer model can be utilized to develop numerous other spintronic devices, including GMR and SOT-based devices.

Acknowledgment

This work benefited from state aid managed by the National Research Agency under France 2030 with the reference "ANR-22-EXSP-0006".

References

[1] G. Wang, Y. Zhang, J. Wang, Z. Zhang, K. Zhang, Z. Zheng, J.-O. Klein, D. Ravelosona, Y. Zhang, and W. Zhao, "Compact modeling of perpendicular-magnetic-anisotropy double-barrier magnetic tunnel junction with enhanced thermal stability recording structure," *IEEE Transactions on Electron Devices*, vol. 66, no. 5, pp. 2431–2436, 2019.

[2] S. Tehrani, J. Slaughter, M. Deherrera, B. Engel, N. Rizzo, J. Salter, M. Durlam, R. Dave, J. Janesky, B. Butcher, K. Smith, and G. Grynkewich, "Magnetoresistive random access memory using magnetic tunnel junctions," *Proceedings of the IEEE*, vol. 91, no. 5, pp. 703–714, 2003.

[3] Y. Guillemenet, L. Torres, G. Sassatelli, N. Bruchon, and I. Hassoune, "A non-volatile run-time fpga using thermally assisted switching mrams," in *2008 International Conference on Field Programmable Logic and Applications*, 2008, pp. 421–426.

[4] N. Sakimura, T. Sugibayashi, R. Nebashi, and N. Kasai, "Nonvolatile magnetic flip-flop for standby-power-free socs," *IEEE Journal of Solid-State Circuits*, vol. 44, no. 8, pp. 2244–2250, 2009.

[5] H. Farkhani, M. Tohidi, S. Farkhani, J. K. Madsen, and F. Moradi, "A low-power high-speed spintronics-based neuromorphic computing system using real-time tracking method," *IEEE Journal on Emerging and Selected Topics in Circuits and Systems*, vol. 8, no. 3, pp. 627–638, 2018.

[6] J.-B. Kammerer, M. Madec, and L. Hébrard, "Compact modeling of a magnetic tunnel junction—part i: Dynamic magnetization model," *IEEE Transactions on Electron Devices*, vol. 57, no. 6, pp. 1408–1415, 2010.

[7] M. Madec, J.-B. Kammerer, F. Pregaldiny, L. Hebrard, and C. Lallement, "Compact modeling of magnetic tunnel junction," in *2008 Joint 6th International IEEE Northeast Workshop on Circuits and Systems and TAISA Conference*, 2008, pp. 229–232.

[8] M. Madec, J.-B. Kammerer, and L. Hébrard, "Compact modeling of a magnetic tunnel junction—part ii: Tunneling current model," *IEEE Transactions on Electron Devices*, vol. 57, no. 6, pp. 1416–1424, 2010.

[9] K. Jabeur, G. Prenat, G. Di Pendina, L. D. Buda-Prejbeanu, I. Prejbeanu, and B. Dieny, "Compact model of a three-terminal mram device based on spin orbit torque switching," in *2013 International Semiconductor Conference Dresden - Grenoble (ISCDG)*, 2013, pp. 1–4.

[10] Z. Lei, G. Li, W. Egelhoff, P. Lai, and P. Pong, "Review of noise sources in magnetic tunnel junction sensors," *IEEE Transactions on Magnetics*, vol. 47, no. 3, pp. 602–612, mar 2011.

[11] K. Sekiguchi, T. Arakawa, Y. Yamauchi, K. Chida, M. Yamada, H. Takahashi, D. Chiba, K. Kobayashi, and T. Ono, "Observation of full shot noise in CoFeB/MgO/CoFeB-based magnetic tunneling junctions," *Applied Physics Letters*, vol. 96, no. 25, p. 252504, 06 2010. [Online]. Available: https://doi.org/10.1063/1.3456548

[12] E. R. Nowak, M. B. Weissman, and S. S. P. Parkin, "Electrical noise in hysteretic ferromagnet–insulator–ferromagnet tunnel junctions," *Applied Physics Letters*, vol. 74, no. 4, pp. 600–602, 01 1999. [Online]. Available: https://doi.org/10.1063/1.123158

[13] H. Nicolas, R. C. Sousa, A. Mora-Hernández, I.-L. Prejbeanu, L. Hebrard, J.-B. Kammerer, and J. Pascal, "Conditioning circuits for nanoscale perpendicular spin transfer torque magnetic tunnel junctions as magnetic sensors," *IEEE Sensors Journal*, vol. 23, no. 6, pp. 5670–5680, 2023.